June 27, 2017

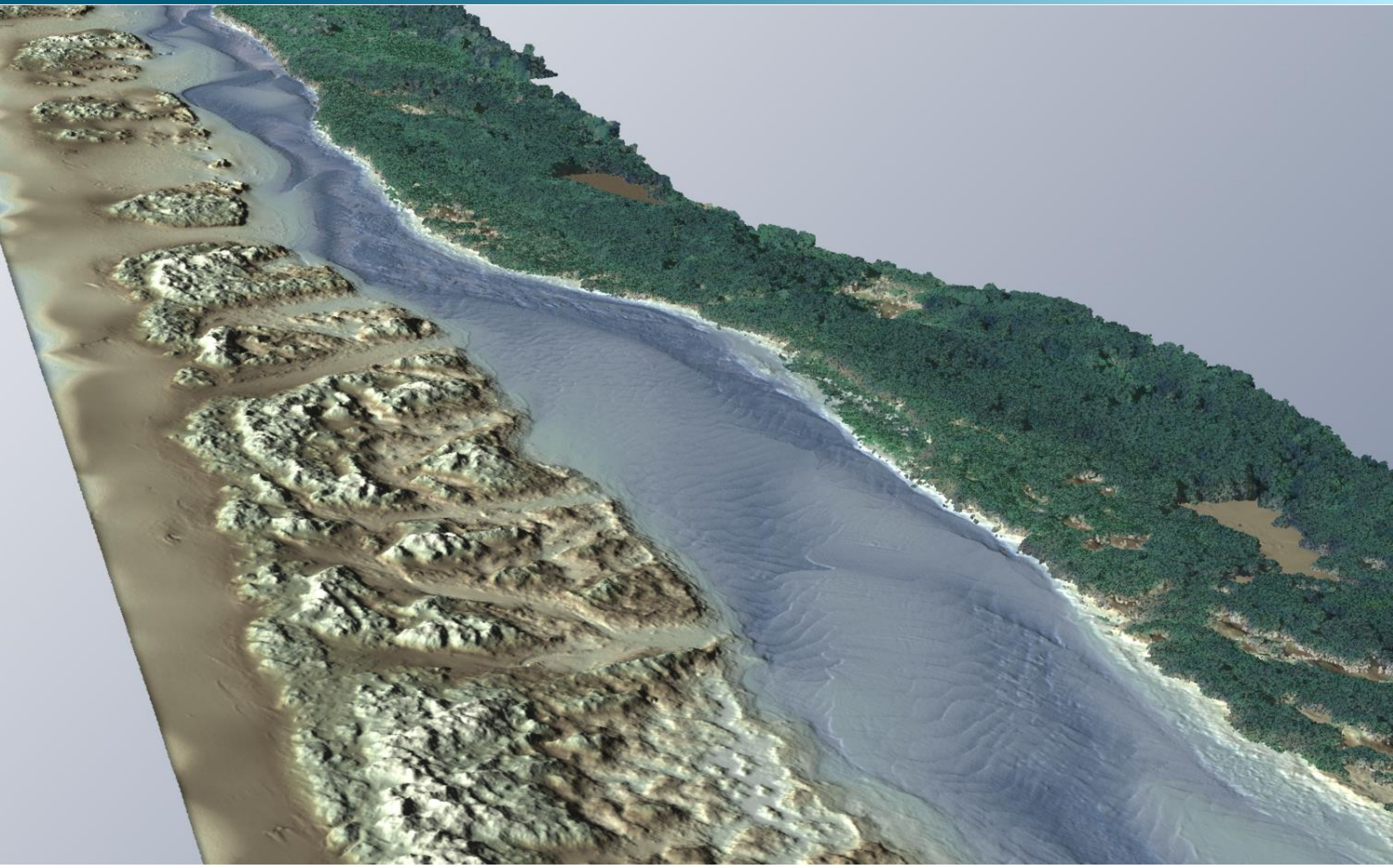

New River, Oregon Topobathymetric LiDAR Technical Data Report

Jacob Edwards
Oregon LiDAR Consortium
Oregon Department of Geology and Mineral Industries
800 NE Oregon St., #28
Portland, OR 97232
PH: 971-673-1557

QSI Corvallis
517 SW 2nd St., Suite 400
Corvallis, OR 97333
PH: 541-752-1204

Table of Contents

Cover Photo: A view looking northeast across the New River, Oregon landscape. The image was created from the LiDAR bare earth model colored by elevation and overlaid with the above-ground point cloud.

INTRODUCTION

This photo taken by QSI acquisition staff shows a view of steep embankment in the New River project area in Oregon.

In late March of 2017, Quantum Spatial (QSI) was contracted by the Oregon LiDAR Consortium (OLC) to collect topobathymetric Light Detection and Ranging (LiDAR) data in the early spring of 2017 for the New River, OR site along the southwestern Oregon coast. The area of interest stretches along New River, which runs parallel with the Oregon coast. Data were collected to aid OLC in assessing the topographic and geophysical properties of the study area along the river's course.

This report accompanies the delivered topobathymetric LiDAR data and documents contract specifications, data acquisition procedures, processing methods, and analysis of the final dataset including LiDAR accuracy and density. Acquisition dates and acreage are shown in Table 1, the project extent is shown in Figure 1, and a complete list of contracted deliverables provided to OLC is shown in Table 2.

Table 1: Acquisition dates, acreage, and data types collected on the New River, OR site

Project Site	Contracted Acres	Buffered Acres	Acquisition Dates	Data Type
New River, OR	1,072	1,916	04/04/2017	Topobathymetric LiDAR

Deliverable Products

Table 2: Products delivered to OLC for the New River, OR site

New River, OR LiDAR Products Projection: UTM Zone 10 North Horizontal Datum: NAD83 (2011) Vertical Datum: NAVD88 (GEOID12A) Units: Meters	
Topobathymetric LiDAR	
Points	LAS v 1.2 • All Classified Returns • Ground Classified Returns by Flight Swath
Rasters	1.0 Meter ESRI Grids • Topobathymetric Bare Earth Model, Interpolated and Clipped[1] • Highest Hit Model • Ground Density Raster 0.5 Meter GeoTiffs • Intensity Images
Vectors	Shapefiles (*.shp) • Contracted and Buffered Site Boundaries • LiDAR Tile Index • DEM Tile Index • Flight Trajectories • Water's Edge Breaklines • Bathymetric Coverage • Ground Survey Points

[1] *Topobathymetric bare earth model clipped using a shape derived from areas that lacked topobathymetric ground returns (see* Topobathymetric DEMs*, page 12)*

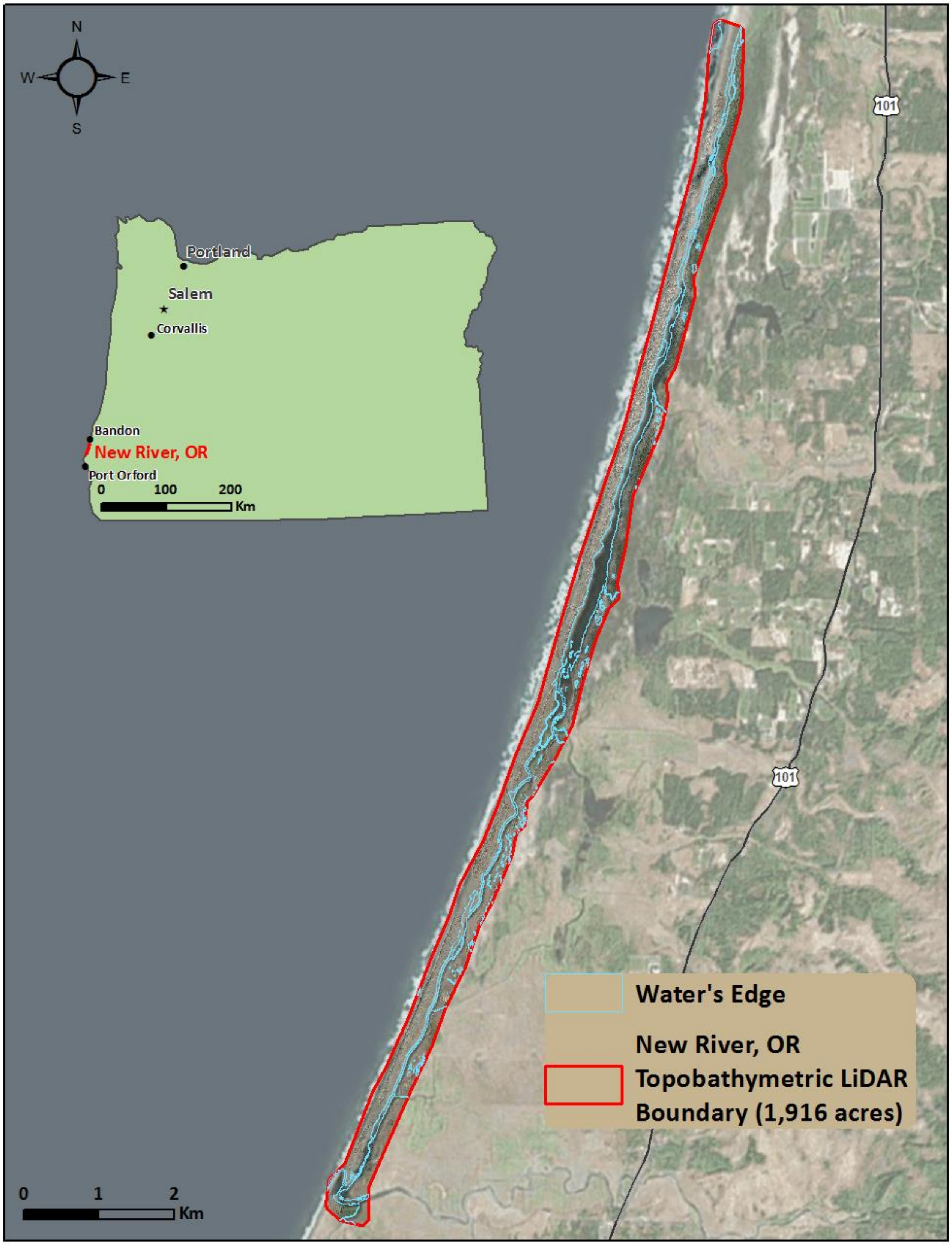

Figure 1: Location map of the New River, OR site in Oregon

QSI's Cessna Caravan

Sensor Selection: the Riegl VQ-880-G

The Riegl VQ-880-G was selected as the hydrographic airborne laser scanner for the New River, OR project based on fulfillment of several considerations deemed necessary for effective mapping of the project site. The instrument's high repetition pulse rate, high scanning speed, small laser footprint, and wide field of view allow for seamless high resolution coverage of topographic and bathymetric surfaces. A short laser pulse length makes the instrument ideal for shallow-water systems as it allows for the discrimination between water surface and bathymetric surface, critical to mapping near-shore and shallow and dynamic environments such as the New River in Oregon. Although the Riegl VQ-880-G also has a built-in NIR scanner, the green wavelength laser scanner has proven very effective at capturing both topographic and bathymetric surfaces and easily captured the targeted point density; therefore, QSI utilized only the green wavelength returns for the New River, OR LiDAR project. Data from the NIR sensor was used exclusively for water surface mapping critical to refraction of the bathymetric data. Sensor specifications and settings for the New River, OR acquisition are displayed in Table 3.

Planning

In preparation for data collection, QSI reviewed the project area and developed a specialized flight plan to ensure complete coverage of the study area at the target point density of ≥6.0 points/m^2. Acquisition parameters including orientation relative to terrain, flight altitude, pulse rate, scan angle, and ground speed were adapted to optimize flight paths and flight times while meeting all contract specifications.

Factors such as satellite constellation availability and weather windows must be considered during the planning stage. Any weather hazards or conditions affecting the flight were continuously monitored due to their potential impact on the daily success of airborne and ground operations. In addition, logistical considerations including private property access and potential air space restrictions and water clarity were reviewed (Figure 2).

Figure 2: Photos taken by QSI acquisition staff, displaying water clarity conditions along the river banks within the New River, OR project area.

Port Orford, OR 9431647 Tidal Data Print View

NOAA/NOS/CO-OPS
Tide Predictions at 9431647, Port Orford OR
From 2017/04/04 12:00 AM LST/LDT to 2017/04/04 11:59 PM LST/LDT

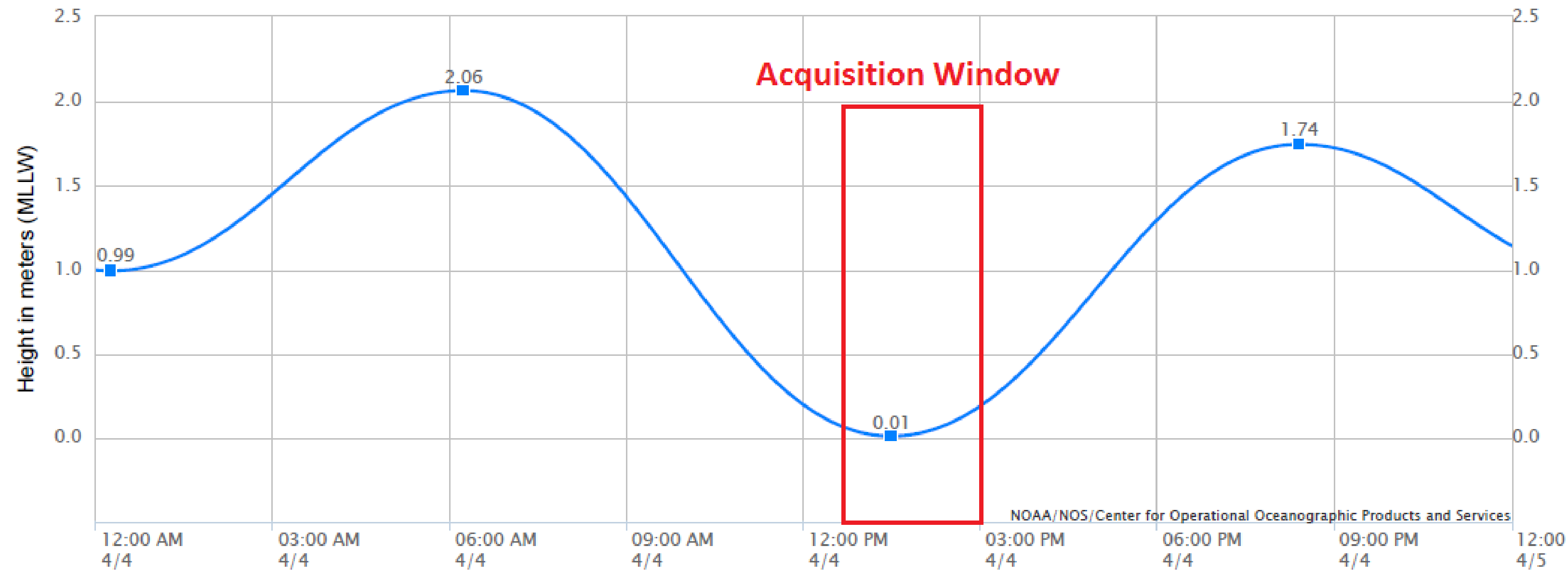

Note: The interval is High/Low, the solid blue line depicts a curve fit between the high and low values and approximates the segments between.
Disclaimer: These data are based upon the latest information available as of the date of your request, and may differ from the published tide tables.

High/Low Tide Prediction Data Listing

Station Name: Port Orford, OR
Action: Daily
Product: Tide Predictions
Start Date & Time: 2017/4/4 12:00 AM
End Date & Time: 2017/4/4 11:59 PM

Source: NOAA/NOS/CO-OPS
Prediction Type: Harmonic
Datum: MLLW
Height Units: Meters
Time Zone: LST/LDT

Date	Day	Time	Hgt	Time	Hgt	Time	Hgt	Time	Hgt
2017/04/04	Tue	12:16 AM	0.99 L	06:14 AM	2.06 H	1:29 PM	0.01 L	8:24 PM	1.74 H

Figure 3: NOAA tidal data on day of topobathymetric LiDAR acquisition (04/04/2017)

Airborne Topobathymetric LiDAR Survey

The LiDAR survey was accomplished using a Riegl VQ-880-G topobathymetric sensor in a Cessna Caravan. The Riegl VQ-880-G uses a green wavelength (ʎ=532 nm) laser that can collect high resolution vegetation and topography data, as well as penetrating the water surface with minimal spectral absorption by water. The recorded waveform enables range measurements for all discernible targets for a given pulse. The typical number of returns digitized from a single pulse range from 1 to 7 for the New River, OR project area. It is not uncommon for some types of surfaces (e.g., dense vegetation or water) to return fewer pulses to the LiDAR sensor than the laser originally emitted. The discrepancy between first return and overall delivered density will vary depending on terrain, land cover, and the prevalence of water bodies. All discernible laser returns were processed for the output dataset. Table 3 summarizes the settings used to yield an average pulse density of ≥6 pulses/m^2 over the New River, OR project area.

Table 3: LiDAR specifications and survey settings

LiDAR Survey Settings & Specifications	
Acquisition Dates	04/04/2017
Aircraft Used	Cessna Caravan
Sensor	Riegl VQ-880-G
Survey Altitude (AGL)	372 m
Swath Width	290 m
Target Pulse Rate	245 kHz
Pulse Mode	Multi Pulse in Air (MPiA)
Laser Pulse Footprint Diameter	26 cm
Mirror Scan Rate	50 Hz
Field of View	40º
GPS Baselines	≤13 nm
GPS PDOP	≤3.0
GPS Satellite Constellation	≥6
Maximum Returns	Unlimited
Intensity	16-bit
Resolution/Density	Average 6 pulses/m2
Accuracy	RMSEZ ≤ 15 cm

All areas were surveyed with an opposing flightline side-lap of ≥50% (≥100% overlap) in order to reduce laser shadowing and increase surface laser painting. To accurately solve for laser point position (geographic coordinates x, y, and z), the positional coordinates of the airborne sensor and the attitude of the aircraft were recorded continuously throughout the LiDAR data collection mission. Position of the aircraft was measured twice per second (2 Hz) by an onboard differential GPS unit, and aircraft attitude was measured 200 times per second (200 Hz) as pitch, roll, and yaw (heading) from an onboard inertial measurement unit (IMU). To allow for post-processing correction and calibration, aircraft and sensor position and attitude data are indexed by GPS time.

Ground Control

Existing NGS Monument

Ground control surveys, including monumentation, ground control points (GCPs), and ground survey points (GSPs), were conducted to support the airborne acquisition. Ground control data were used to geospatially correct the aircraft positional coordinate data, while GSPs were used to perform accuracy assessments on final LiDAR data.

Monumentation

The spatial configuration of ground survey monuments provided redundant control within 13 nautical miles of the mission areas for LiDAR flights. Monuments were also used for collection of GCPs and GSPs using real time kinematic (RTK) and post processed kinematic (PPK) survey techniques.

Monument locations were selected with consideration for satellite visibility, field crew safety, and optimal location for GCP and GSP coverage. QSI utilized two existing NGS monuments for the New River, OR LiDAR project (Table 4, Figure 4). QSI's professional land surveyor, Evon Silvia (ORPLS#81104) oversaw and certified the utilization of all monuments.

Table 4: Monuments established for the New River, OR acquisition. Coordinates are on the NAD83 (2011) datum, epoch 2010.00.

Monument ID	Latitude	Longitude	Ellipsoid (meters)
OA0762	42° 59' 02.96235"	-124° 25' 21.54995"	7.905
Q_609	42° 54' 59.84256"	-124° 27' 06.88290"	-6.221

To correct the continuously recorded onboard measurements of the aircraft position, QSI concurrently conducted multiple static Global Navigation Satellite System (GNSS) ground surveys (1 Hz recording frequency) over each monument. During post-processing, the static GPS data were triangulated with nearby Continuously Operating Reference Stations (CORS) using the Online Positioning User Service (OPUS[2]) for precise positioning. Multiple independent sessions over the same monument were processed to confirm antenna height measurements and to refine position accuracy.

Monuments were established according to the national standard for geodetic control networks, as specified in the Federal Geographic Data Committee (FGDC) Geospatial Positioning Accuracy Standards for geodetic networks.[3] This standard provides guidelines for classification of monument quality at the 95% confidence interval as a basis for comparing the quality of one control network to another. The monument rating for this project is shown in Table 5.

[2] OPUS is a free service provided by the National Geodetic Survey to process corrected monument positions. http://www.ngs.noaa.gov/OPUS.

[3] Federal Geographic Data Committee, Geospatial Positioning Accuracy Standards (FGDC-STD-007.2-1998). Part 2: Standards for Geodetic Networks, Table 2.1, page 2-3. http://www.fgdc.gov/standards/projects/FGDC-standards-projects/accuracy/part2/chapter2

Table 5: Federal Geographic Data Committee monument rating for network accuracy

Direction	Rating
1.96 * St Dev $_{NE}$:	0.020 m
1.96 * St Dev $_{z}$:	0.020 m

For the New River, OR LiDAR project, the monument coordinates contributed no more than 2.8 cm of positional error to the geolocation of the final ground survey points and LiDAR, with 95% confidence.

Ground Control Points and Ground Survey Points

Ground control points (GCPs) and ground survey points (GSPs) were collected using real time kinematic (RTK) and post-processed kinematic (PPK) survey techniques. A Trimble R7 base unit was positioned at a nearby monument to broadcast a kinematic correction to a roving Trimble R8 GNSS receiver. All GCP and GSP measurements were made during periods with a Position Dilution of Precision (PDOP) of ≤ 3.0 with at least six satellites in view of the stationary and roving receivers. When collecting RTK and PPK data, the rover records data while stationary for five seconds, then calculates the pseudorange position using at least three one-second epochs. Relative errors for any point must be less than 1.5 cm horizontal and 2.0 cm vertical in order to be accepted. See Table 6 for Trimble unit specifications.

GCPs and GSPs were collected in areas where good satellite visibility was achieved on paved roads and other hard surfaces such as grave, packed dirt roads, or compacted silt. Measurements were not taken on highly reflective surfaces such as center line stripes or lane markings on roads due to the increased noise seen in the laser returns over these surfaces. GCPs and GSPs were collected within as many flightlines as possible; however, distribution depended on ground access constraints and monument locations and may not be equitably distributed throughout the study area (Figure 4).

Table 6: Trimble equipment identification

Receiver Model	Antenna	OPUS Antenna ID	Use
Trimble R7 GNSS	Zephyr GNSS Geodetic Model 2 RoHS	TRM57971.00	Static
Trimble R8	Integrated Antenna R8 Model 2	TRM_R8_GNSS	Rover

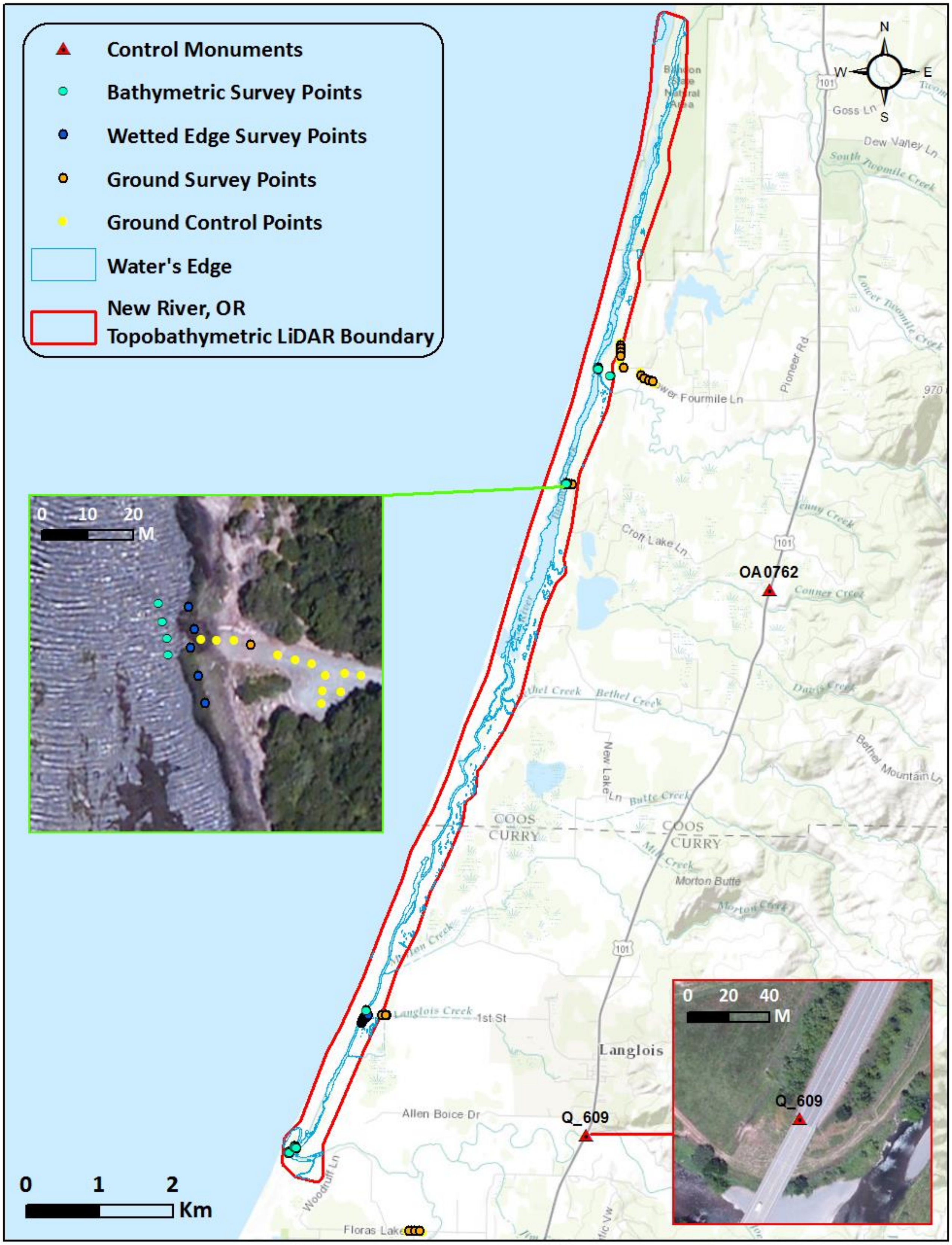

Figure 4: Ground survey map

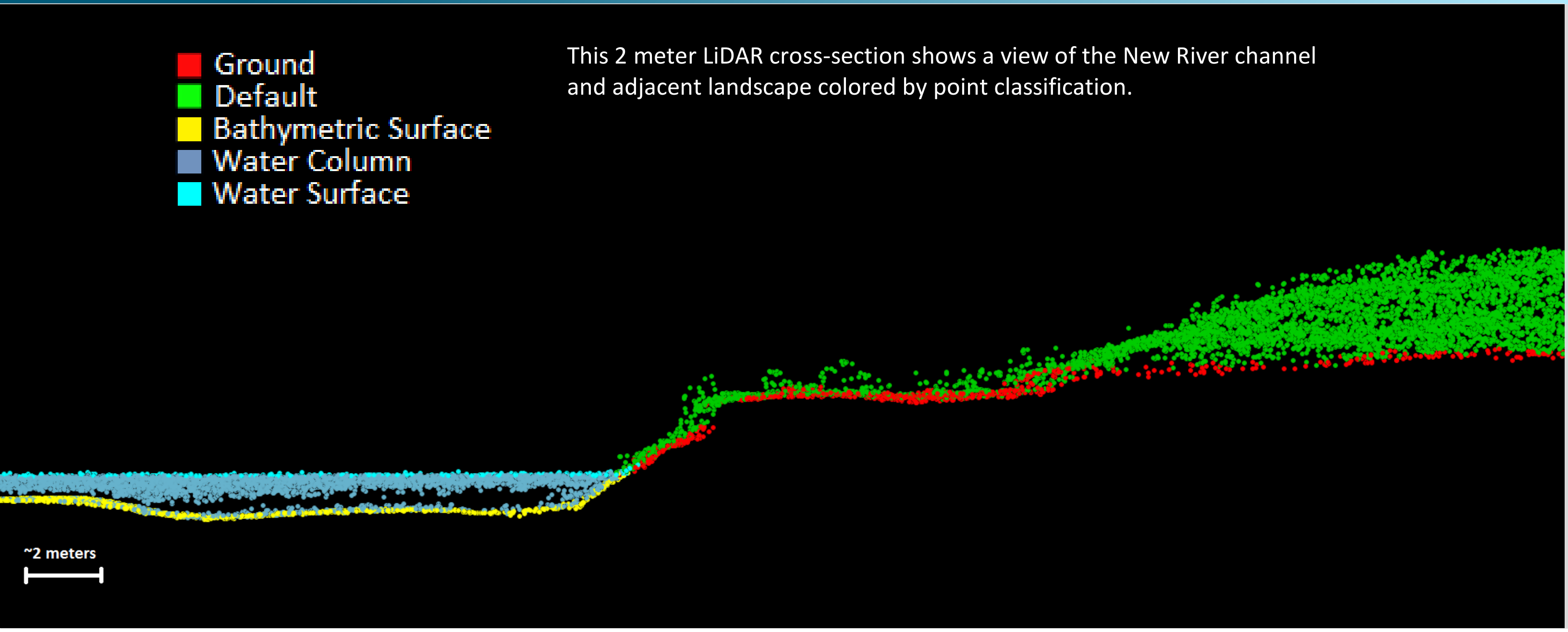

This 2 meter LiDAR cross-section shows a view of the New River channel and adjacent landscape colored by point classification.

Topobathymetric LiDAR Data

Upon completion of data acquisition, QSI processing staff initiated a suite of automated and manual techniques to process the data into the requested deliverables. Processing tasks included GPS control computations, smoothed best estimate trajectory (SBET) calculations, kinematic corrections, calculation of laser point position, sensor and data calibration for optimal relative and absolute accuracy, and LiDAR point classification (Table 7). Riegl's RiProcess software was used to facilitate bathymetric return processing. Once bathymetric points were differentiated, they were spatially corrected for refraction through the water column based on the angle of incidence of the laser. QSI refracted water column points using QSI's proprietary LAS processing software, LAS Monkey. The resulting point cloud data were classified using both manual and automated techniques. Processing methodologies were tailored for the landscape. Brief descriptions of these tasks are shown in Table 8.

Table 7: ASPRS LAS classification standards applied to the New River, OR dataset

Classification Number	Classification Name	Classification Description
1	Default/Unclassified	Laser returns that are not included in the ground class, composed of vegetation and anthropogenic features.
2	Ground	Laser returns that are determined to be ground using automated and manual cleaning algorithms.
25	Water Column	Refracted Riegl sensor returns that are determined to be water using automated and manual cleaning algorithms.
26	Bathymetric Bottom	Refracted Riegl sensor returns that fall within the water's edge breakline which characterize the submerged topography.
27	Water Surface	Green LiDAR returns that are near the water's surface.

Table 8: LiDAR processing workflow

LiDAR Processing Step	Software Used
Resolve kinematic corrections for aircraft position data using kinematic aircraft GPS and static ground GPS data. Develop a smoothed best estimate of trajectory (SBET) file that blends post-processed aircraft position with sensor head position and attitude recorded throughout the survey.	Waypoint Inertial Explorer v.8.6 POSPac MMS v7.1 SP3
Calculate laser point position by associating SBET position to each laser point return time, scan angle, intensity, etc. Create raw laser point cloud data for the entire survey in *.las (ASPRS v. 1.2) format. Convert data to orthometric elevations by applying a geoid correction.	RiProcess v1.7.2 Waypoint Inertial Explorer v.8.6 TerraMatch v.17
Import raw laser points into manageable blocks (less than 500 MB) to perform manual relative accuracy calibration and filter erroneous points. Classify ground points for individual flightlines.	TerraScan v.17
Using ground classified points per each flightline, test the relative accuracy. Perform automated line-to-line calibrations for system attitude parameters (pitch, roll, heading), mirror flex (scale) and GPS/IMU drift. Calculate calibrations on ground classified points from paired flightlines and apply results to all points in a flightline. Use every flightline for relative accuracy calibration.	TerraMatch v.17 RiProcess v1.7.2
Apply refraction correction to all subsurface returns.	LAS Monkey 2.2.6 (QSI proprietary)
Classify resulting data to ground and other client designated ASPRS classifications (Table 7). Assess statistical absolute accuracy via direct comparisons of ground classified points to ground control survey data.	TerraScan v.17 TerraModeler v.17
Generate bare earth models as triangulated surfaces. Generate highest hit models as a surface expression of all classified points. Export all surface models as ESRI GRIDs at a 1 meter pixel resolution.	TerraScan v.17 TerraModeler v.17 ArcMap v. 10.2.2
Correct intensity values for variability and export intensity images of all returns as GeoTIFFs at a 0.5 meter pixel resolution.	ArcMap v. 10.2.2 Las Product Creator 1.5 (QSI proprietary)

Bathymetric Refraction

The water surface model used for refraction is generated using NIR points within the breaklines defining the water's edge. Points are filtered and edited to obtain the most accurate representation of the water surface and are used to create a water surface model TIN. A tin model is preferable to a raster based water surface model to obtain the most accurate angle of incidence during refraction. The refraction processing is done using Las Monkey; QSI's proprietary LiDAR processing tool. After refraction, the points are compared against bathymetric control points to assess accuracy.

LiDAR Derived Products

Because hydrographic laser scanners penetrate the water surface to map submerged topography, this affects how the data should be processed and presented in derived products from the LiDAR point cloud. The following discusses certain derived products that vary from the traditional (NIR) specification and delivery format.

Topobathymetric DEMs

Bathymetric bottom returns can be limited by depth, water clarity, and bottom surface reflectivity. Water clarity and turbidity affects the depth penetration capability of the green wavelength laser with returning laser energy diminishing by scattering throughout the water column. Additionally, the bottom surface must be reflective enough to return remaining laser energy back to the sensor at a detectable level. Although the predicted depth penetration range of the Riegl VQ-880-G sensor is 1.5 Secchi depths on brightly reflective surfaces, it is not unexpected to have no bathymetric bottom returns in turbid or non-reflective areas.

As a result, creating digital elevation models (DEMs) presents a challenge with respect to interpolation of areas with no returns. Traditional DEMs are "unclipped", meaning areas lacking ground returns are interpolated from neighboring ground returns (or breaklines in the case of hydro-flattening), with the assumption that the interpolation is close to reality. In bathymetric modeling, these assumptions are prone to error because a lack of bathymetric returns can indicate a change in elevation that the laser can no longer map due to increased depths. The resulting void areas may suggest greater depths, rather than similar elevations from neighboring bathymetric bottom returns. Therefore, QSI created a water polygon with bathymetric coverage to delineate areas with successfully mapped bathymetry. This shapefile was used to control the extent of the delivered clipped topobathymetric model to avoid false triangulation (interpolation from TIN'ing) across areas in the water with no bathymetric returns.

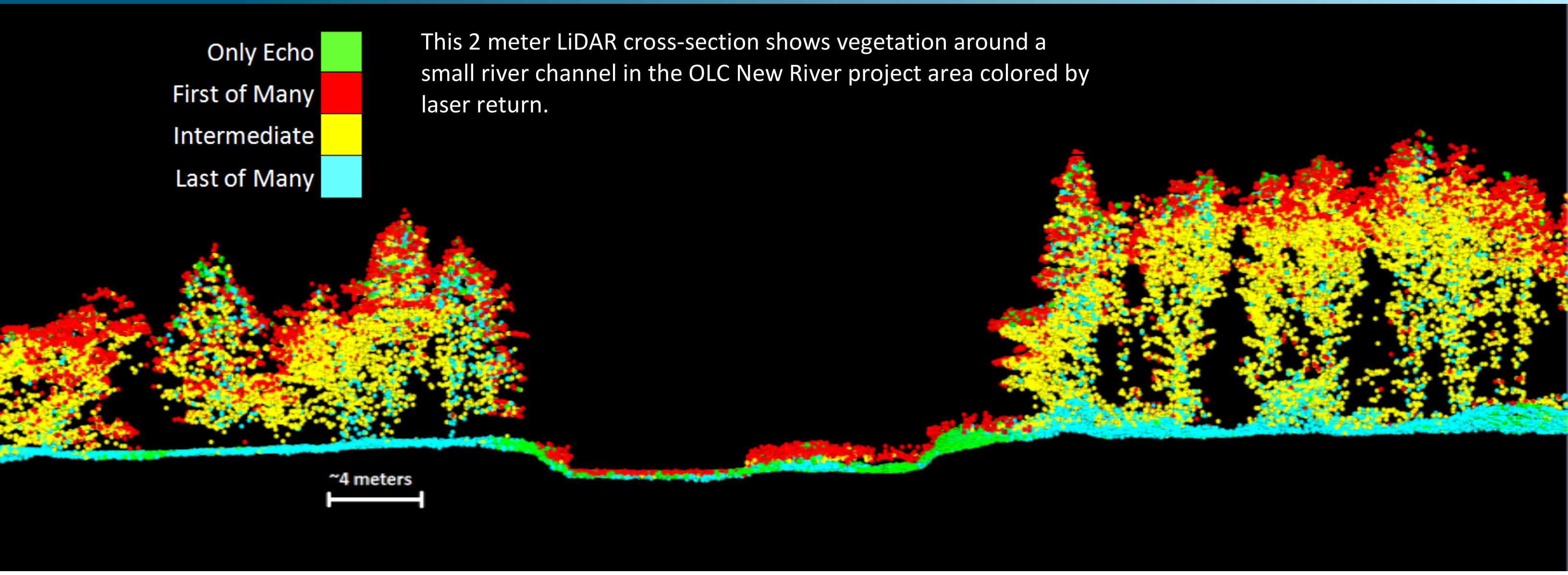

This 2 meter LiDAR cross-section shows vegetation around a small river channel in the OLC New River project area colored by laser return.

Bathymetric LiDAR

An underlying principle for collecting hydrographic LiDAR data is to survey near-shore areas that can be difficult to collect with other methods, such as multi-beam sonar, particularly over large areas. In order to determine the capability and effectiveness of the bathymetric LiDAR, several parameters were considered; bathymetric coverage, bathymetric return density, and spatial accuracy.

Mapped Bathymetry

The specified depth penetration range of the Riegl VQ-880-G sensor is 1.5x the secchi depth; therefore, bathymetry data below 1.5x the secchi depth at the time of acquisition is not to be expected. To assist in evaluating performance results of the sensor, a polygon layer was created to delineate areas where bathymetry was successfully mapped.

This shapefile was used to control the extent of the delivered clipped topobathymetric model and to avoid false triangulation across areas in the water with no returns. Insufficiently mapped areas were identified by triangulating bathymetric bottom points with an edge length maximum of 4.56 meters. This ensured all areas of no returns (> 9 m^2), were identified as data voids.

LiDAR Point Density

First Return Point Density

The acquisition parameters were designed to acquire an average first-return density of 6 points/m². First return density describes the density of pulses emitted from the laser that return at least one echo to the system. Multiple returns from a single pulse were not considered in first return density analysis. Some types of surfaces (e.g., breaks in terrain, water and steep slopes) may have returned fewer pulses than originally emitted by the laser.

First returns typically reflect off the highest feature on the landscape within the footprint of the pulse. In forested or urban areas the highest feature could be a tree, building or power line, while in areas of unobstructed ground, the first return will be the only echo and represents the bare earth surface.

The average first-return density for the New River, OR project was 34.12 points/m². The statistical and spatial distributions of all first return densities per 100 m x 100 m cell are portrayed in Figure 5 and Figure 7.

Table 9: Average First Return LiDAR point densities

First Return Type	Point Density
First Returns	34.12 points/m²

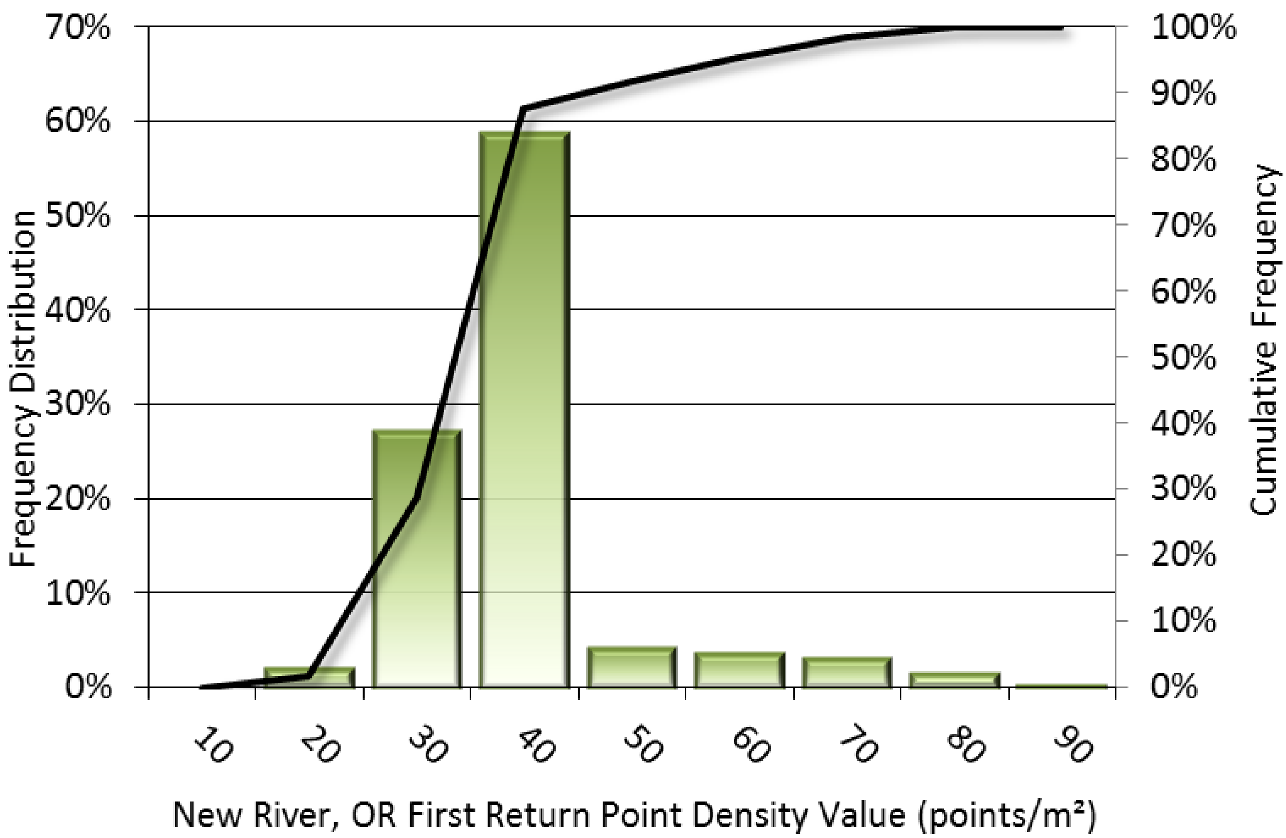

Figure 5: Frequency distribution of first return densities per 100 x 100 m cell

Bathymetric and Ground Classified Point Densities

The density of ground classified LiDAR returns and bathymetric bottom returns were also analyzed for this project. Terrain character, land cover, and ground surface reflectivity all influenced the density of ground surface returns. In vegetated areas, fewer pulses may have penetrated the canopy, resulting in lower ground density. Similarly, the density of bathymetric bottom returns was influenced by turbidity, depth, and bottom surface reflectivity. In turbid areas, fewer pulses may have penetrated the water surface, resulting in lower bathymetric density.

The ground and bathymetric bottom classified density of LiDAR data for the New River, OR project was 12.85 points/m^2. The statistical and spatial distributions ground classified and bathymetric bottom return densities per 100 m x 100 m cell are portrayed in Figure 6 and Figure 7.

Additionally, for the New River, OR project, density values of only bathymetric bottom returns were calculated for areas considered successfully mapped. Areas lacking bathymetric returns were not considered in calculating an average density value. Within the successfully mapped area, a bathymetric bottom return density of 16.14 points/m^2 was achieved.

Table 10: Average Ground and Bathymetric Classified LiDAR point densities

Classification	Point Density
Ground and Bathymetric Bottom Classified Returns	12.85 points/m^2
Bathymetric Bottom Classified Returns	16.14 points/m^2

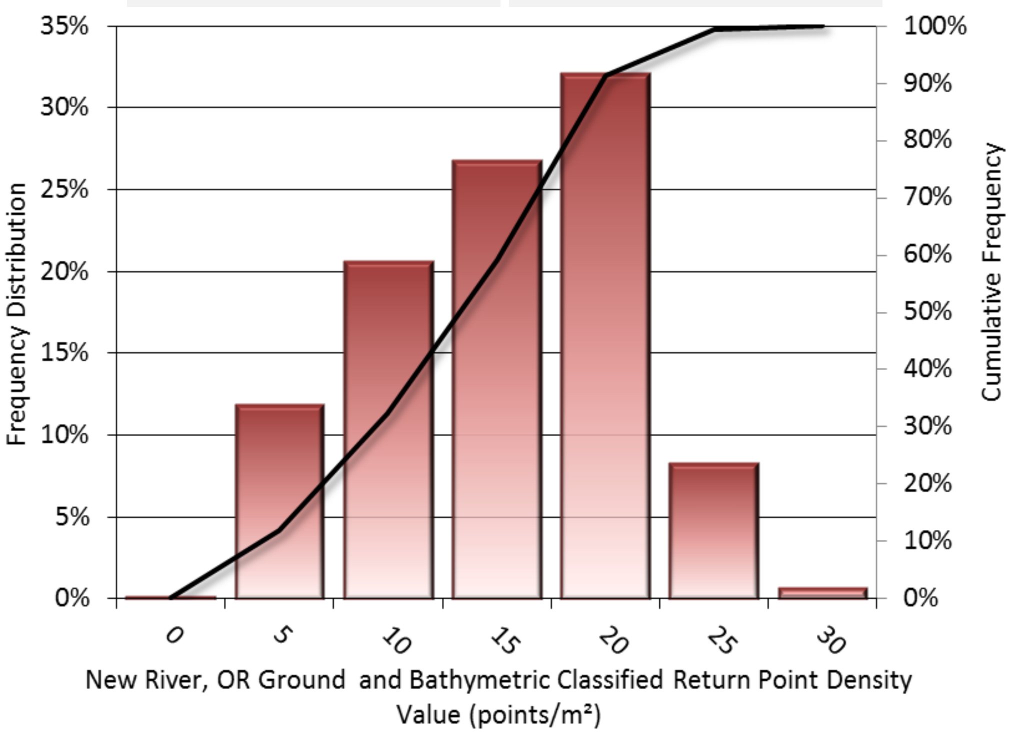

Figure 6: Frequency distribution of bathymetric and ground classified return densities per 100 m x 100 m cell

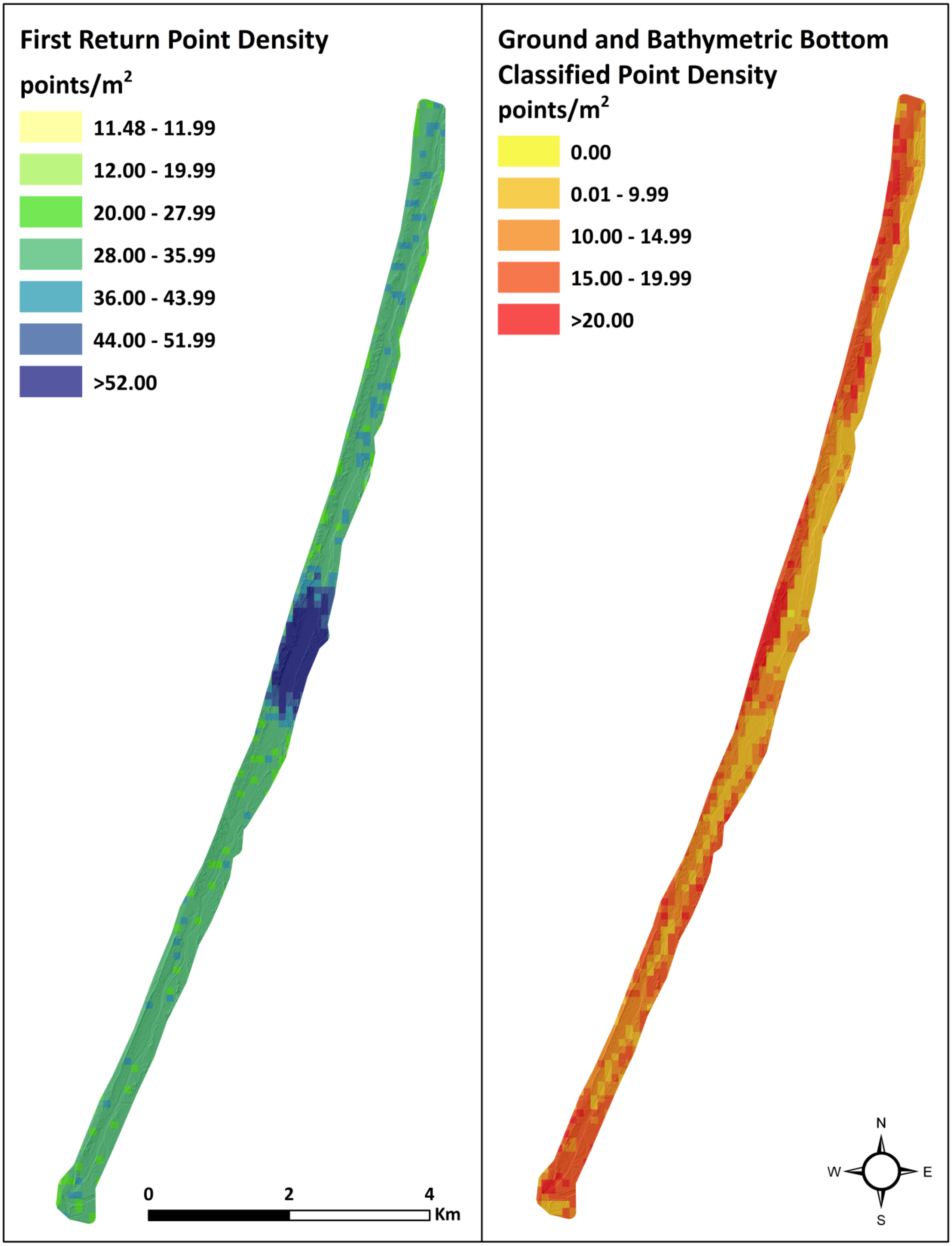

Figure 7: First return and ground density map for the New River, OR site (100 m x 100 m cells)

LiDAR Accuracy Assessments

The accuracy of the LiDAR data collection can be described in terms of absolute accuracy (the consistency of the data with external data sources) and relative accuracy (the consistency of the dataset with itself). See Appendix A for further information on sources of error and operational measures used to improve relative accuracy.

LiDAR Absolute Accuracy

Absolute accuracy was assessed using Non-Vegetated Vertical Accuracy (NVA) reporting designed to meet guidelines presented in the FGDC National Standard for Spatial Data Accuracy[4]. NVA compares known ground survey point data collected on open, bare earth surfaces with level slope (<20°) to the triangulated surface generated by the LiDAR points. NVA is a measure of the accuracy of LiDAR point data in open areas where the LiDAR system has a high probability of measuring the ground surface and is evaluated at the 95% confidence interval (1.96 * RMSE), as shown in Table 11.

The mean and standard deviation (sigma σ) of divergence of the ground surface model from ground survey point coordinates are also considered during accuracy assessment. These statistics assume the error for x, y and z is normally distributed, and therefore the skew and kurtosis of distributions are also considered when evaluating error statistics. For the New River, OR survey, 19 ground survey points were withheld in total resulting in a non-vegetated vertical accuracy of 0.034 meters (Figure 8).

QSI also assessed absolute accuracy using 177 ground control points. Although these points were used in the calibration and post-processing of the LiDAR point cloud, they may still provide a good indication of the overall accuracy of the LiDAR dataset, and therefore have been provided in Table 11 and Figure 9.

Table 11: Absolute accuracy results

Absolute Accuracy		
	Ground Survey Points (NVA)	**Ground Control Points**
Sample	19 points	177 points
NVA (1.96*RMSE)	0.034 m	0.031 m
Average	-0.002 m	-0.004 m
Median	0.001 m	-0.003 m
RMSE	0.017 m	0.016 m
Standard Deviation (1σ)	0.018 m	0.015 m

[4] Federal Geographic Data Committee, Geospatial Positioning Accuracy Standards (FGDC-STD-007.3-1998). Part 3: National Standard for Spatial Data Accuracy. http://www.fgdc.gov/standards/projects/FGDC-standards-projects/accuracy/part3/chapter3

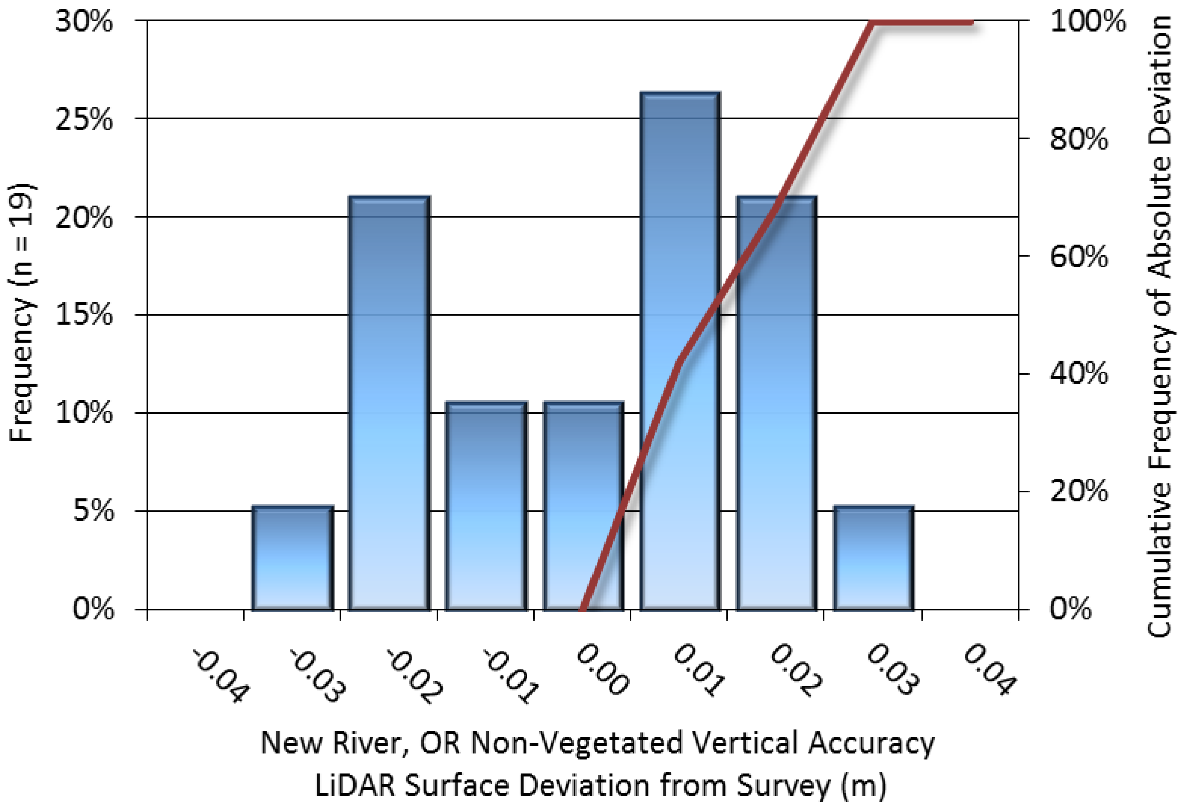

Figure 8: Frequency histogram for LiDAR surface deviation from ground survey point positions

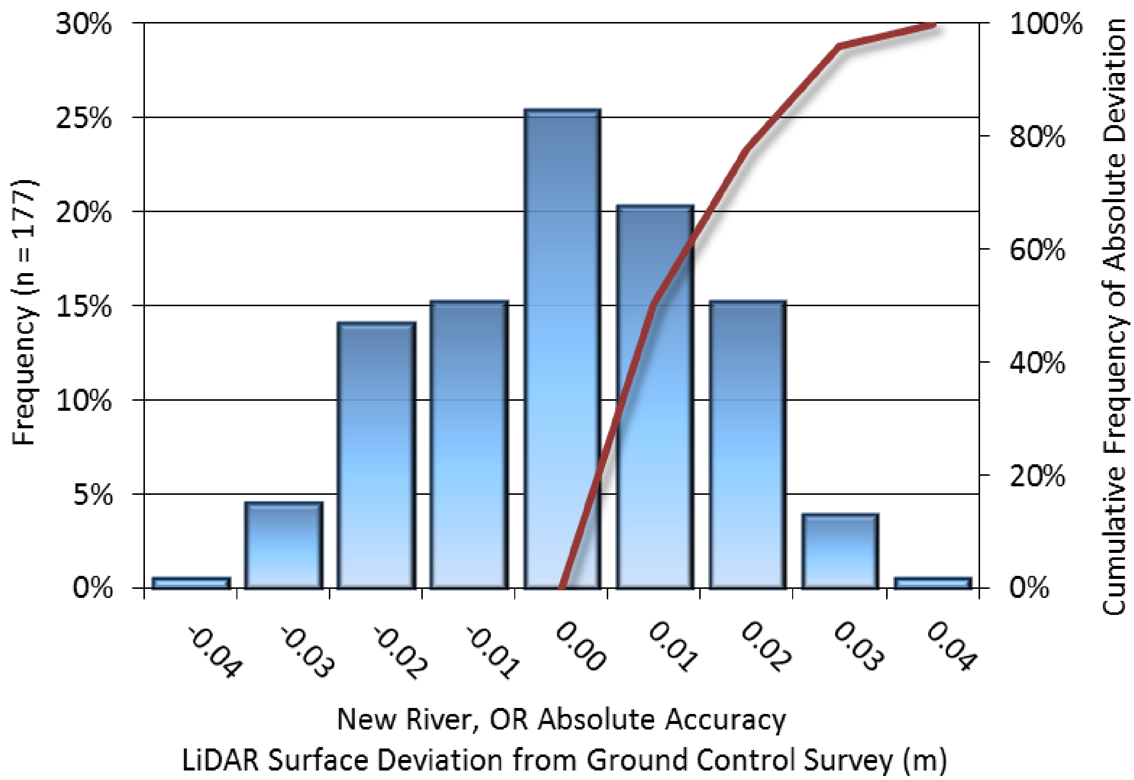

Figure 9: Frequency histogram for LiDAR surface deviation from ground control point positions

LiDAR Topobathymetric Absolute Accuracies

Additionally, topobathymetric check points were collected in order to assess vertical accuracies of the topobathymetric surface in and around the river. These check points were collected along the water's edge and submerged within the water for evaluation against the topobathymetric ground surface. The wetted edge check points yielded a vertical accuracy of 0.061 meters while the submerged bathymetric check points had a vertical accuracy of 0.104 meters (Table 12, Figure 10 - Figure 11).

Table 12: Topobathymetric absolute accuracy results

Topobathymetric Absolute Accuracy		
	Wetted Edge Check Points	**Submerged Topobathymetric Check Points**
Sample	50 points	94 points
1.96*RMSE	0.057 m	0.104 m
Average	0.013 m	0.030 m
Median	0.003 m	0.029 m
RMSE	0.029 m	0.053 m
Standard Deviation (1σ)	0.026 m	0.044 m

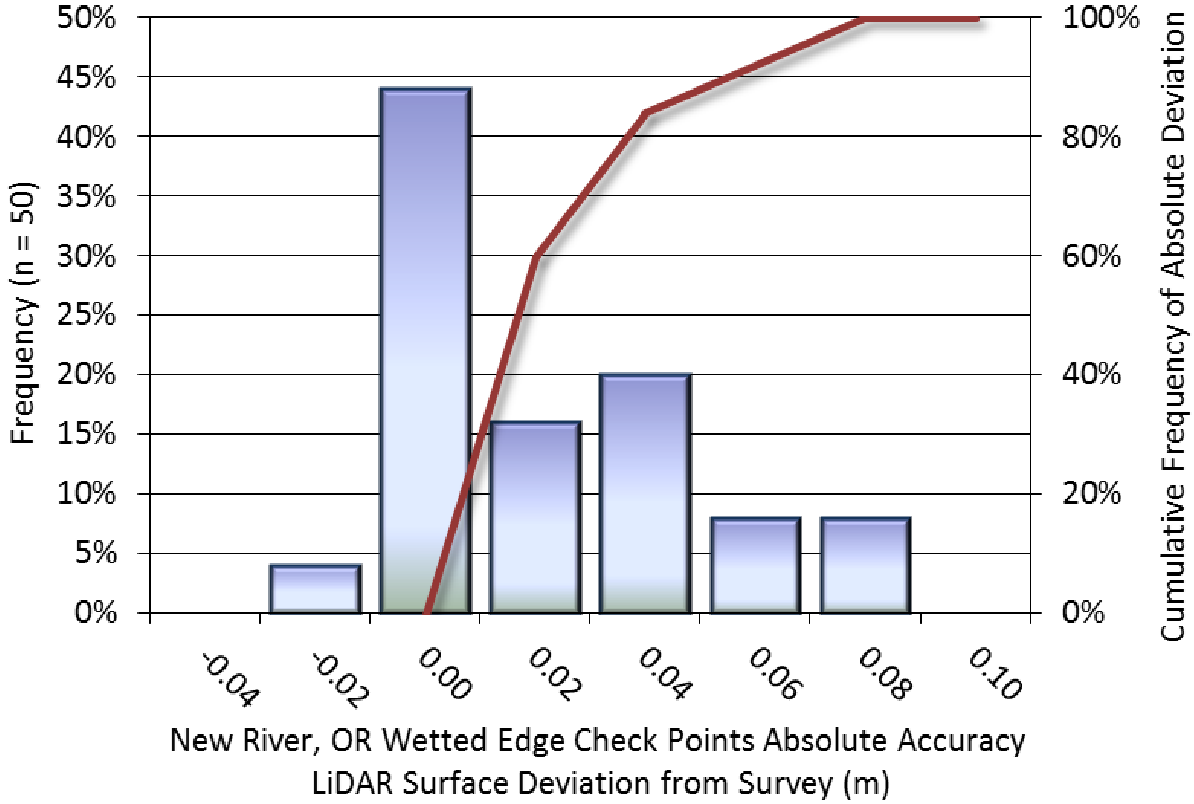

Figure 10: Frequency histogram for LiDAR surface deviation from wetted edge check points

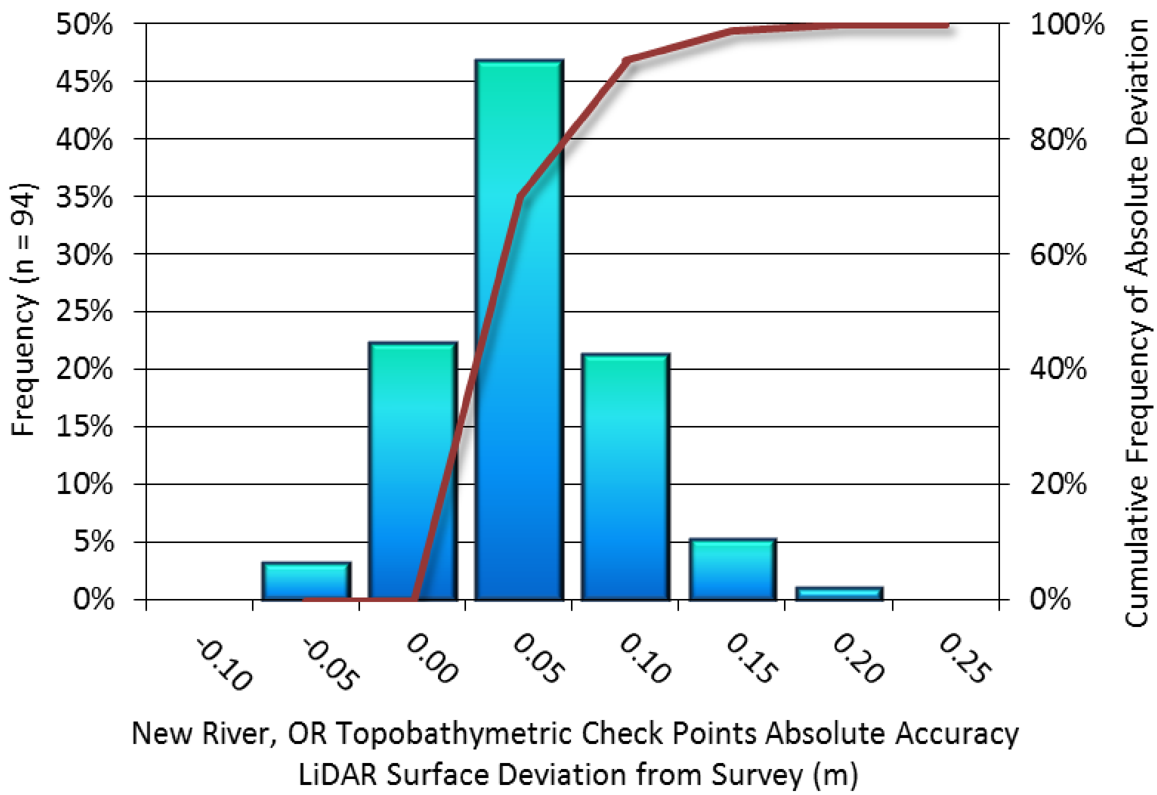

Figure 11: Frequency histogram for LiDAR surface deviation from submerged bathymetric check points

LiDAR Relative Vertical Accuracy

Relative vertical accuracy refers to the internal consistency of the data set as a whole: the ability to place an object in the same location given multiple flightlines, GPS conditions, and aircraft attitudes. When the LiDAR system is well calibrated, the swath-to-swath vertical divergence is low (<0.10 meters). The relative vertical accuracy was computed by comparing the ground surface model of each individual flightline with its neighbors in overlapping regions. The average (mean) line to line relative vertical accuracy for the New River, OR LiDAR project was 0.023 meters (Table 13, Figure 12).

Table 13: Relative accuracy results

Relative Accuracy	
Sample	15 surfaces
Average	0.023 m
Median	0.025 m
RMSE	0.025 m
Standard Deviation (1σ)	0.006 m
1.96σ	0.012 m

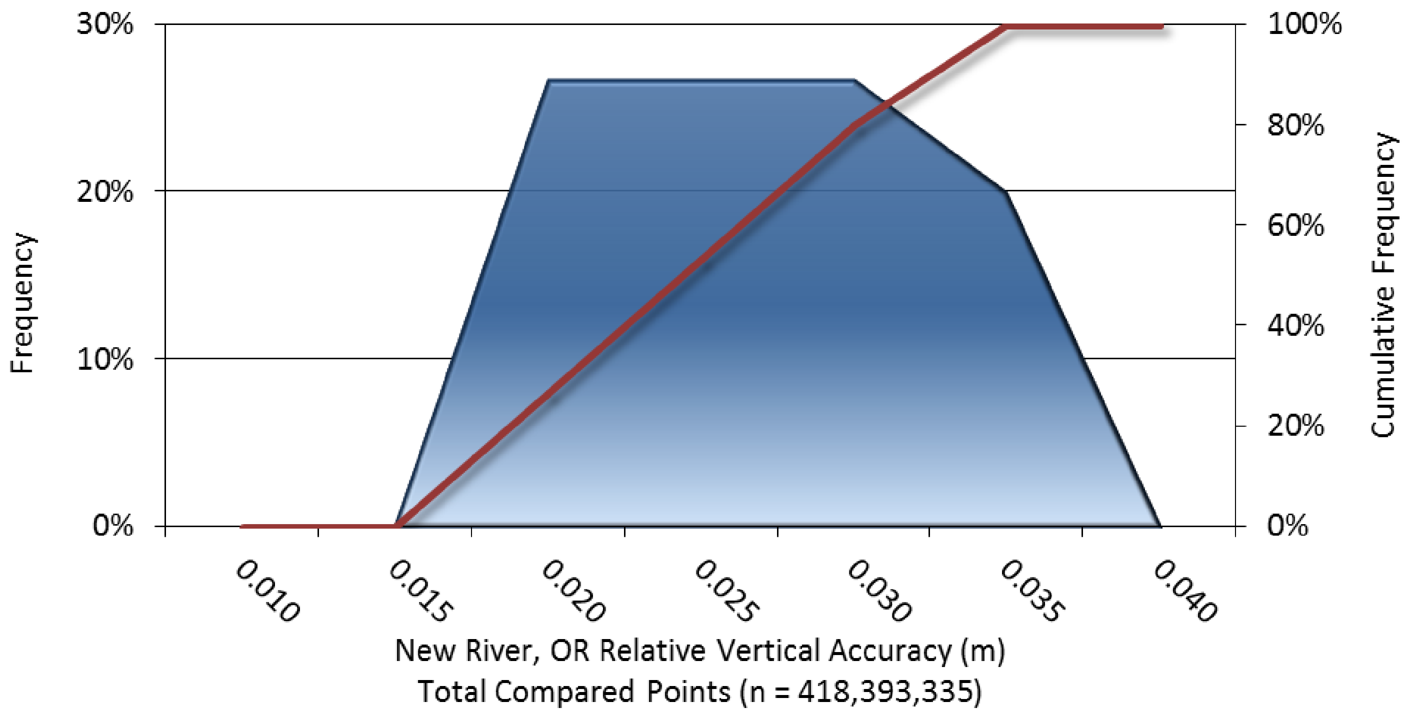

Figure 12: Frequency plot for relative vertical accuracy between flightlines

Quantum Spatial, Inc. provided LiDAR services for the New River, OR project as described in this report.

I, Steven R. Miller, have reviewed the attached report for completeness and hereby state that it is a complete and accurate report of this project.

Steven R. Miller
Steven R. Miller (Jun 27, 2017)

Jun 27, 2017

Steven R. Miller
Project Manager
Quantum Spatial, Inc.

I, Evon P. Silvia, PLS, being duly registered as a Professional Land Surveyor in and by the state of Oregon, hereby certify that the methodologies, static GNSS occupations used during airborne flights, and ground survey point collection were performed using commonly accepted Standard Practices. Field work conducted for this report was conducted between April 4 and 5, 2017.

Accuracy statistics shown in the Accuracy Section of this Report have been reviewed by me and found to meet the "National Standard for Spatial Data Accuracy".

Evon P. Silvia

Jun 27, 2017

Evon P. Silvia, PLS
Quantum Spatial, Inc.
Corvallis, OR 97333

REGISTERED
PROFESSIONAL
LAND SURVEYOR

Evon P. Silvia

OREGON
JUNE 10, 2014
EVON P. SILVIA
81104LS

EXPIRES: 06/30/2018

Figure 13: View looking northeast over New River, OR. The image was created from the LiDAR topobathymetric bare earth model overlaid with the above-ground point cloud and the water's edge breaklines. This view comes from the northern section of the project area.

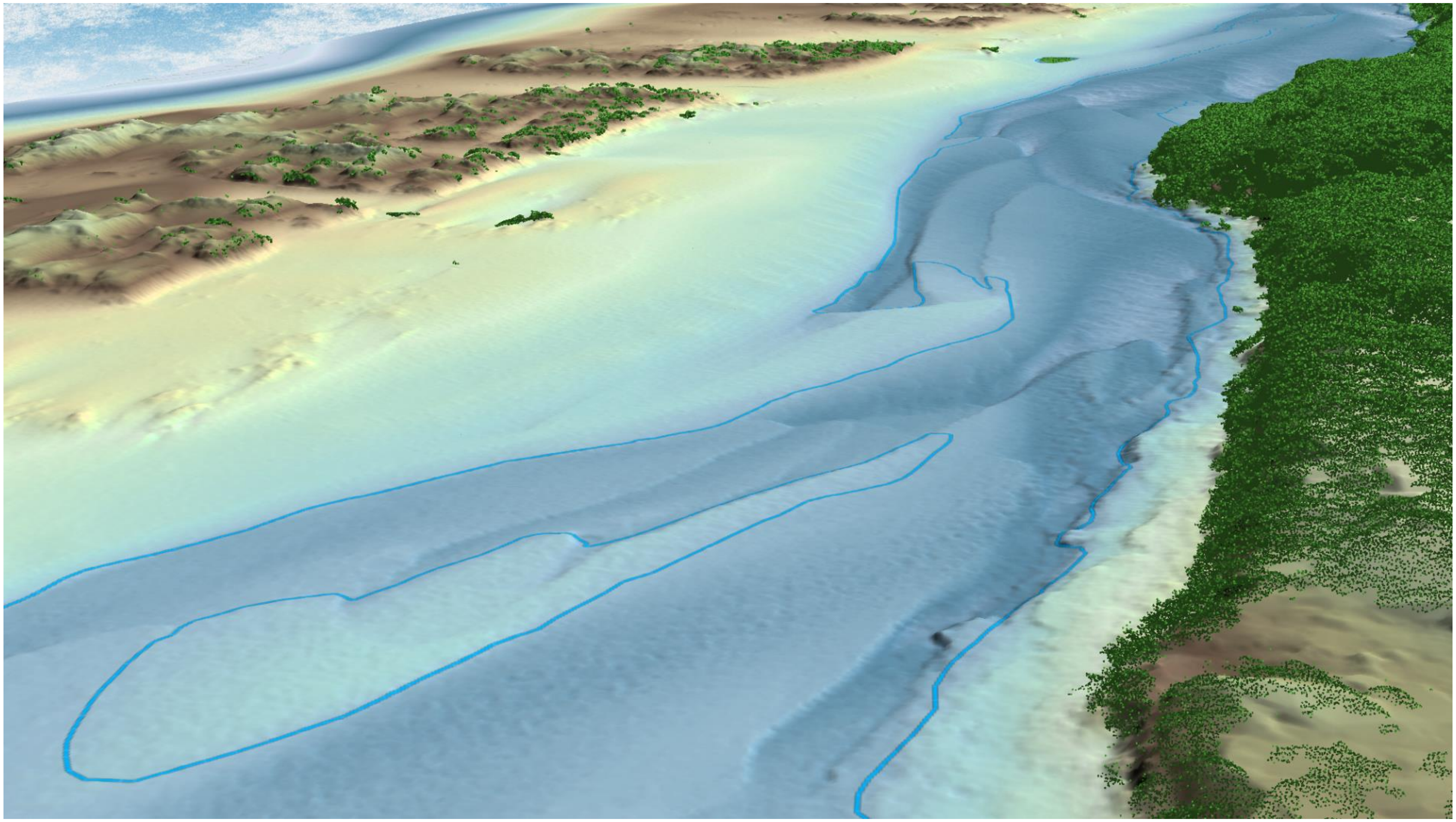

Figure 14: View looking north over New River, OR. The image was created from the LiDAR topobathymetric bare earth model overlaid with the above-ground point cloud and the water's edge breaklines. This view comes from the northern section of the project area.

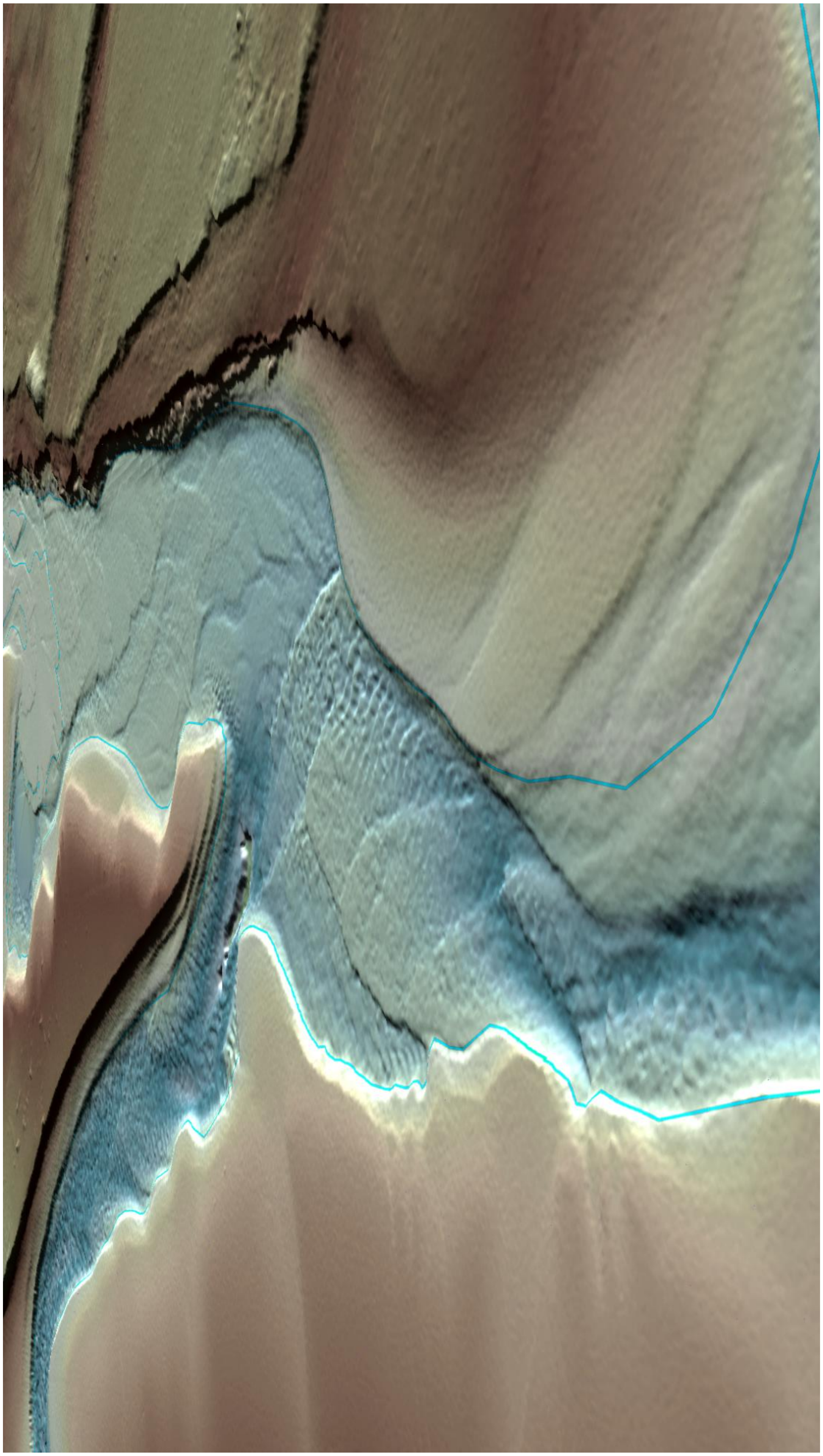

Figure 15: View looking north over New River, OR. The image was created from the LiDAR topobathymetric bare earth model overlaid with the water's edge breaklines. This view comes from the southern section of the project area.

Glossary

1-sigma (σ) Absolute Deviation: Value for which the data are within one standard deviation (approximately 68th percentile) of a normally distributed data set.

1.96 * RMSE Absolute Deviation: Value for which the data are within two standard deviations (approximately 95th percentile) of a normally distributed data set, based on the FGDC standards for Non-Vegetated Vertical Accuracy (NVA) reporting.

Accuracy: The statistical comparison between known (surveyed) points and laser points. Typically measured as the standard deviation (sigma σ) and root mean square error (RMSE).

> **Absolute Accuracy:** The vertical accuracy of LiDAR data is described as the mean and standard deviation (sigma σ) of divergence of LiDAR point coordinates from ground survey point coordinates. To provide a sense of the model predictive power of the dataset, the root mean square error (RMSE) for vertical accuracy is also provided. These statistics assume the error distributions for x, y and z are normally distributed, and thus we also consider the skew and kurtosis of distributions when evaluating error statistics.
>
> **Relative Accuracy:** Relative accuracy refers to the internal consistency of the data set; i.e., the ability to place a laser point in the same location over multiple flightlines, GPS conditions and aircraft attitudes. Affected by system attitude offsets, scale and GPS/IMU drift, internal consistency is measured as the divergence between points from different flightlines within an overlapping area. Divergence is most apparent when flightlines are opposing. When the LiDAR system is well calibrated, the line-to-line divergence is low (<10 cm).
>
> **Root Mean Square Error (RMSE):** A statistic used to approximate the difference between real-world points and the LiDAR points. It is calculated by squaring all the values, then taking the average of the squares and taking the square root of the average.

Data Density: A common measure of LiDAR resolution, measured as points per square meter.

Digital Elevation Model (DEM): File or database made from surveyed points, containing elevation points over a contiguous area. Digital terrain models (DTM) and digital surface models (DSM) are types of DEMs. DTMs consist solely of the bare earth surface (ground points), while DSMs include information about all surfaces, including vegetation and anthropogenic features.

Intensity Values: The peak power ratio of the laser return to the emitted laser, calculated as a function of surface reflectivity.

Nadir: A single point or locus of points on the surface of the earth directly below a sensor as it progresses along its flightline.

Overlap: The area shared between flightlines, typically measured in percent. 100% overlap is essential to ensure complete coverage and reduce laser shadows.

Pulse Rate (PR): The rate at which laser pulses are emitted from the sensor; typically measured in thousands of pulses per second (kHz).

Pulse Returns: For every laser pulse emitted, the number of wave forms (i.e., echos) reflected back to the sensor. Portions of the wave form that return first are the highest element in multi-tiered surfaces such as vegetation. Portions of the wave form that return last are the lowest element in multi-tiered surfaces.

Real-Time Kinematic (RTK) Survey: A type of surveying conducted with a GPS base station deployed over a known monument with a radio connection to a GPS rover. Both the base station and rover receive differential GPS data and the baseline correction is solved between the two. This type of ground survey is accurate to 1.5 cm or less.

Post-Processed Kinematic (PPK) Survey: GPS surveying is conducted with a GPS rover collecting concurrently with a GPS base station set up over a known monument. Differential corrections and precisions for the GNSS baselines are computed and applied after the fact during processing. This type of ground survey is accurate to 1.5 cm or less.

Scan Angle: The angle from nadir to the edge of the scan, measured in degrees. Laser point accuracy typically decreases as scan angles increase.

Native LiDAR Density: The number of pulses emitted by the LiDAR system, commonly expressed as pulses per square meter.

Relative Accuracy Calibration Methodology:

Manual System Calibration: Calibration procedures for each mission require solving geometric relationships that relate measured swath-to-swath deviations to misalignments of system attitude parameters. Corrected scale, pitch, roll and heading offsets were calculated and applied to resolve misalignments. The raw divergence between lines was computed after the manual calibration was completed and reported for each survey area.

Automated Attitude Calibration: All data were tested and calibrated using TerraMatch automated sampling routines. Ground points were classified for each individual flightline and used for line-to-line testing. System misalignment offsets (pitch, roll and heading) and scale were solved for each individual mission and applied to respective mission datasets. The data from each mission were then blended when imported together to form the entire area of interest.

Automated Z Calibration: Ground points per line were used to calculate the vertical divergence between lines caused by vertical GPS drift. Automated Z calibration was the final step employed for relative accuracy calibration.

LiDAR accuracy error sources and solutions:

Type of Error	Source	Post Processing Solution
GPS (Static/Kinematic)	Long Base Lines	None
	Poor Satellite Constellation	None
	Poor Antenna Visibility	Reduce Visibility Mask
Relative Accuracy	Poor System Calibration	Recalibrate IMU and sensor offsets/settings
	Inaccurate System	None
Laser Noise	Poor Laser Timing	None
	Poor Laser Reception	None
	Poor Laser Power	None
	Irregular Laser Shape	None

Operational measures taken to improve relative accuracy:

Low Flight Altitude: Terrain following was employed to maintain a constant above ground level (AGL). Laser horizontal errors are a function of flight altitude above ground (about 1/3000th AGL flight altitude).

Focus Laser Power at narrow beam footprint: A laser return must be received by the system above a power threshold to accurately record a measurement. The strength of the laser return (i.e., intensity) is a function of laser emission power, laser footprint, flight altitude and the reflectivity of the target. While surface reflectivity cannot be controlled, laser power can be increased and low flight altitudes can be maintained.

Reduced Scan Angle: Edge-of-scan data can become inaccurate. The scan angle was reduced to a maximum of $\pm 20^{o}$ from nadir, creating a narrow swath width and greatly reducing laser shadows from trees and buildings.

Quality GPS: Flights took place during optimal GPS conditions (e.g., 6 or more satellites and PDOP [Position Dilution of Precision] less than 3.0). Before each flight, the PDOP was determined for the survey day. During all flight times, a dual frequency DGPS base station recording at 1 second epochs was utilized and a maximum baseline length between the aircraft and the control points was less than 13 nm at all times.

Ground Survey: Ground survey point accuracy (<1.5 cm RMSE) occurs during optimal PDOP ranges and targets a minimal baseline distance of 4 miles between GPS rover and base. Robust statistics are, in part, a function of sample size (n) and distribution. Ground survey points are distributed to the extent possible throughout multiple flightlines and across the survey area.

50% Side-Lap (100% Overlap): Overlapping areas are optimized for relative accuracy testing. Laser shadowing is minimized to help increase target acquisition from multiple scan angles. Ideally, with a 50% side-lap, the nadir portion of one flightline coincides with the swath edge portion of overlapping flightlines. A minimum of 50% side-lap with terrain-followed acquisition prevents data gaps.

Opposing Flightlines: All overlapping flightlines have opposing directions. Pitch, roll and heading errors are amplified by a factor of two relative to the adjacent flightline(s), making misalignments easier to detect and resolve.